Supporting Information (SI) for

Bicarbonate anion coordination assisted CO_2 capture by using urea-morpholine hybrid receptors in water

Zhiwen Sun, Ji Wang, Qingling Nie, Na Li, Zhihua Liu, Xiao-Juan Yang, Wei Zhao,* and Biao Wu

Key Laboratory of Medicinal Molecule Science and Pharmaceutics Engineering of Ministry of Industry and Information Technology, School of Chemistry and Chemical Engineering, Beijing Institute of Technology, Beijing 10248, China.

E-mail: zhaochem@bit.edu.cn

Table of contents

S1. General Information

All starting materials and solvents were obtained from commercial sources (Beijing InnoChem, Aladdin, Macklin Science & Technology Co., Ltd.), which were used without further purification. ^{1}H spectra was recorded on Bruker AVANCE AV II-400/500 MHz spectrometer at 298 K. ^{1}H NMR chemical shifts were reported according to residual solvent peaks (^{1}H NMR: 2.50 ppm for DMSO-d_6).

S2. Synthetic Procedures of Receptors

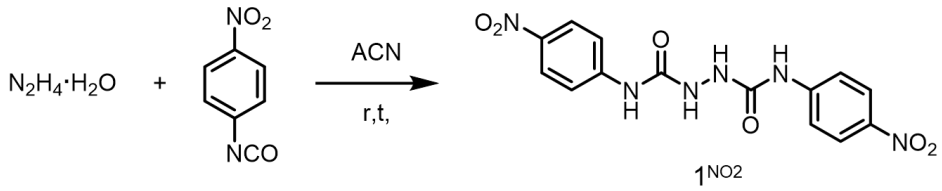

Scheme S1 Synthetic procedure of making **1^{NO2}** according to previous studies (*J. Incl. Phenom. Macrocycl. Chem.* (2011) 69:101–106).

Receptor 1^{NO2}: At room temperature, place p-nitrophenyl isocyanate (0.65 g, 3.96 mmol, 2.2 equivalents) in a 50 mL double-neck round-bottom flask with dry acetonitrile (25 mL). 80% hydrazine hydrate solution (0.1 g, 2.0 mmol, 1.0 equiv.) in dry acetonitrile (15 mL) was added dropwise. The mixture was stirred at the same temperature for 4 hours. Then, solids were separated by filtration. The obtained yellow powder was further washed by acetonitrile and diethyl ether 3 times (30 mL). A pale-yellow solid powder was obtained as receptor **1^{NO2}** (Yield: 0.46 g, 80 %). The compound was characterized and confirmed by ^{1}H NMR according to previously reported data (J Incl Phenom Macrocycl Chem (2011) 69:101–106). ^{1}H NMR (400 MHz, DMSO-d_6) δ = 9.61 (s, 1H), 8.45 (s, 1H), 8.17 (dd, J1 = 12 Hz, J = 4 Hz, 2H), 7.78 (d, J = 7.5 Hz, 2H). ^{13}C NMR (101 MHz, DMSO-d_6, 298 K) δ = 155.6, 147.1, 142.0, 125.2, 118.7.

Figure S1 ^{1}H NMR spectrum of $\mathbf{1^{NO2}}$ (400 MHz, 298 K, DMSO-d_6).

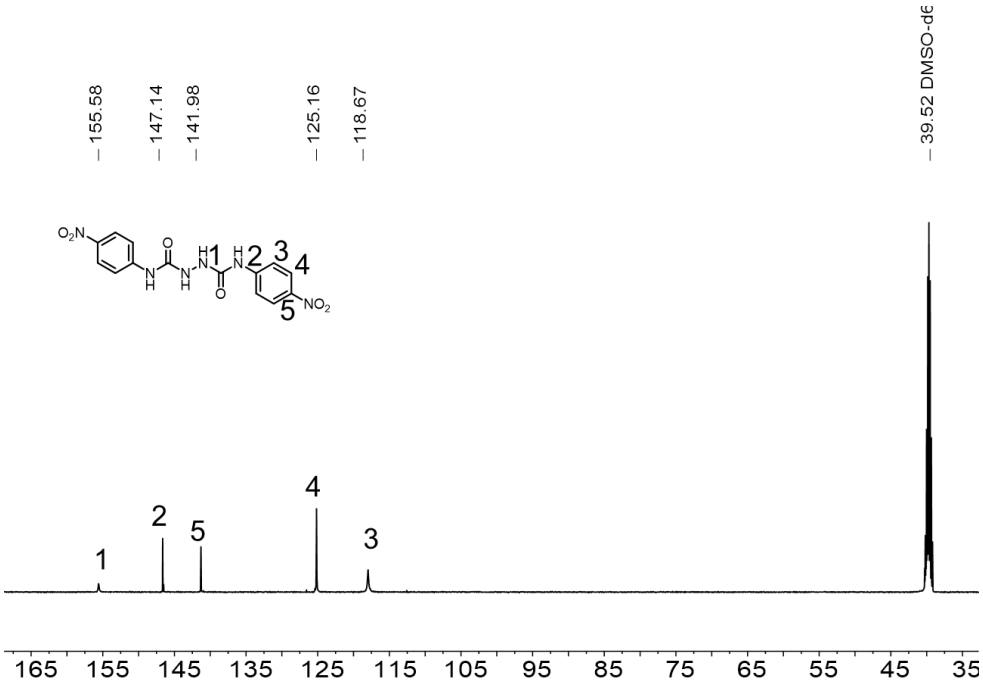

Figure S2 ^{13}C NMR spectrum of $\mathbf{1^{NO2}}$ (101 MHz, 298 K, DMSO-d_6).

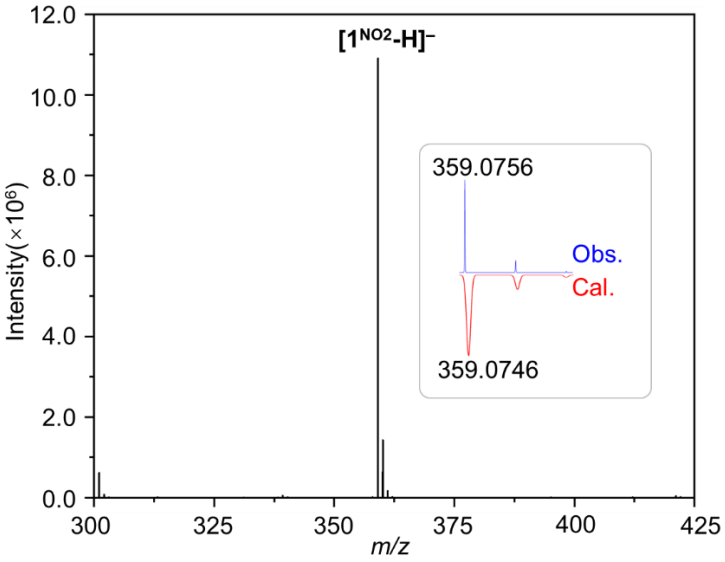

Figure S3 HR-ESI-QTOF Mass spectrum for **1**^{NO2}.

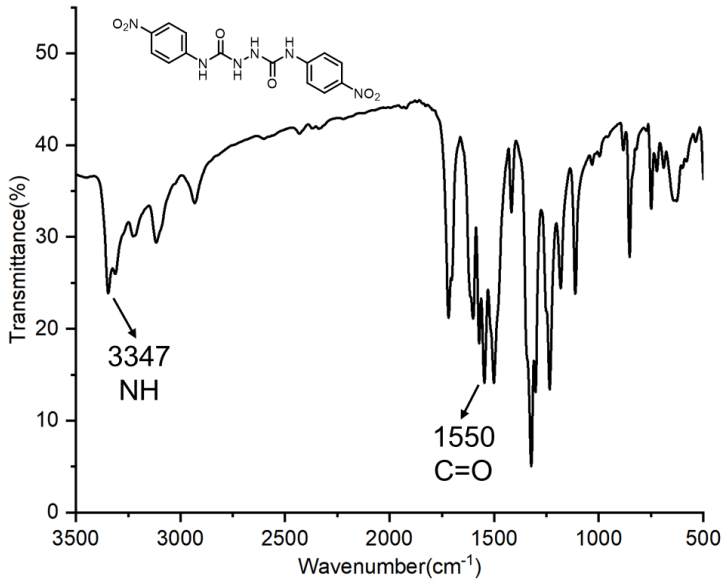

Figure S4 FT-IR spectra of **1**^{NO2}.

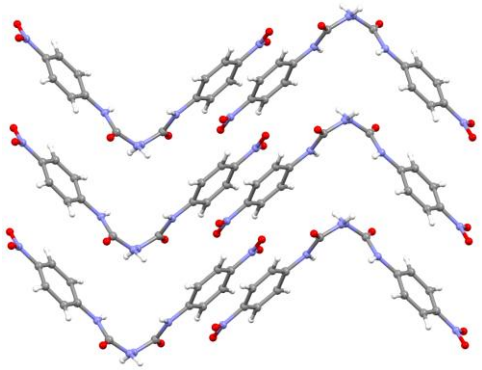

Figure S5 Single crystal structure of **1**^{NO2}. CCDC reference number 2517602.

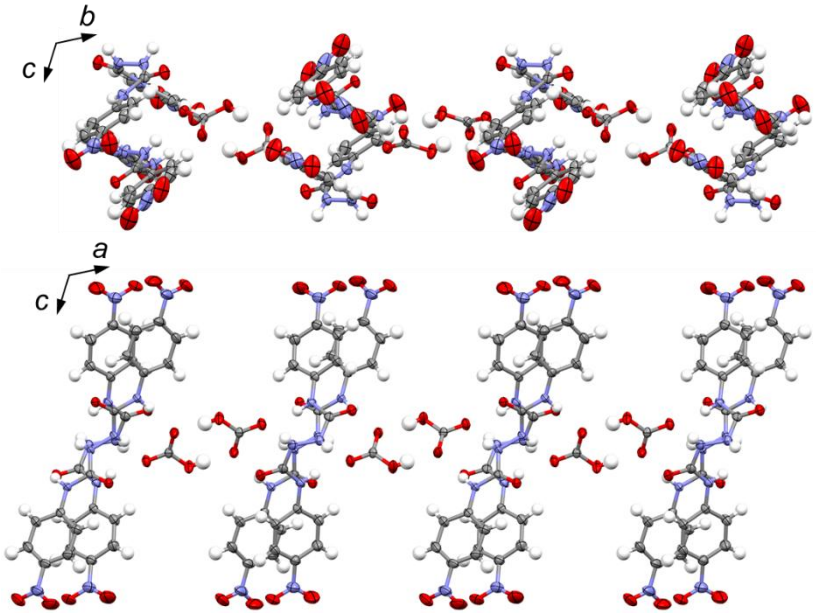

Figure S6 Single crystal structure of $\mathbf{1}^{\mathbf{NO2}}$-$HCO_3^-$. Solvent molecules and tetramethylammonium cations (TMA^+) are omitted for clarity. Their anion binding structures with urea units are shown in the middle boxes. The HCO_3^- anion dimerizes through two complementary hydrogen bonds and interacts with urea units through three hydrogen bonds.

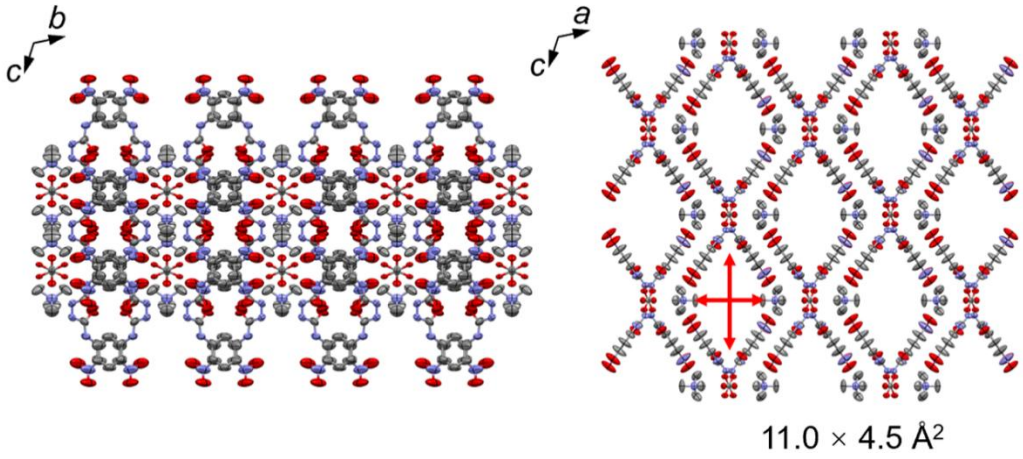

Figure S7 Single crystal structure of $\mathbf{1}^{\mathbf{NO2}}$-$CO_3^{2-}$. Solvent molecules and tetramethylammonium cations (TMA^+) are omitted for clarity. Their anion binding structures with urea units are shown in the middle boxes. The CO_3^{2-} anion is disordered and stabilized by eight hydrogen bonds with four urea unts.

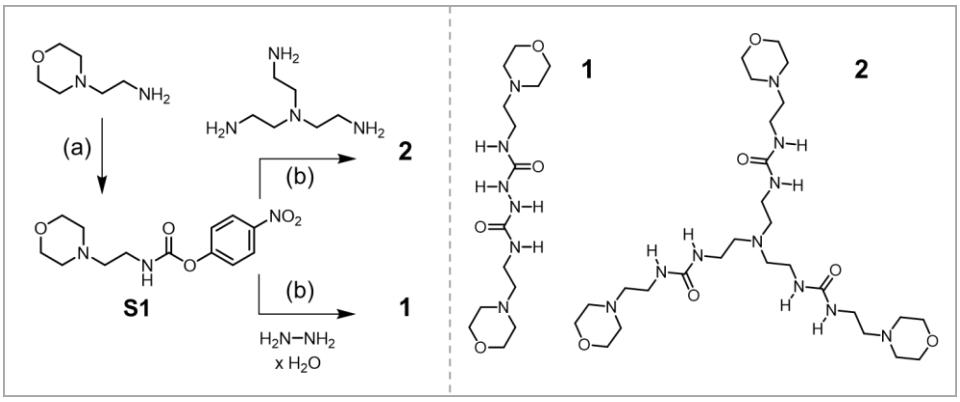

Scheme S2 Synthetic scheme of making receptors.

Compound S1: Under anhydrous and oxygen-free conditions, add DCM solution (50 mL) to a 100 mL two-necked flask. Add 4-nitrophenyl chloroformate (1.41 g, 7.0 mmol, 1.4 eq) and stir magnetically until dissolved.4-(2-Aminoethyl)morpholine (0.7 mL 5.0 mmol, 1.0 eq) was added dropwise (2 drops per second) to the DCM solution. After adding, cool to 0 ℃ and stir for 3 hours. The precipitate was filtered off and washed several times with DCM. Disperse the precipitate into 50 mL of DCM and quickly extract with saturated $NaHCO_3$ solution and the organic phase was separated. The organic layer was rotary-evaporated to yield product as a yellow solid (Yield: 1.0 g, 80 %). TLC-verified pure product is used directly in the next step without NMR characterization.
Receptor 1: Compound a (1.64 g, 5.6 mmol, 2.4 equiv.) was placed in a 500 mL double-necked, round-bottomed flask and suspend in dry acetonitrile (100 mL). The reaction was heated to 50 ℃, and 80% hydrazine hydrate solution (0.15 g, 2.3 mmol, 1.0 equiv.) in dry acetonitrile (15 mL) was added dropwise over 30 min. The mixture was stirred at the same temperature for 6 hours. The reaction mixture was cooled down to room temperature, and the precipitated solids was separated by filtration. The obtained white powder was further washed with acetonitrile and diethyl ether 3 times (30 mL). A white solid powder was yielded as receptor 1(Yield: 1.0 g, 68 %). ^{1}H NMR (400 MHz, DMSO-d_6) δ = 7.66 (s, 1H), 6.22 (s, 1H), 3.55 (s, 4H), 3.12 (d, J = 6.7 Hz, 2H), 2.34 (s, 6H). ^{13}C NMR (101 MHz, DMSO-d_6, 298 K) δ = 160.4, 66.0, 57.2, 52.5, 35.9.

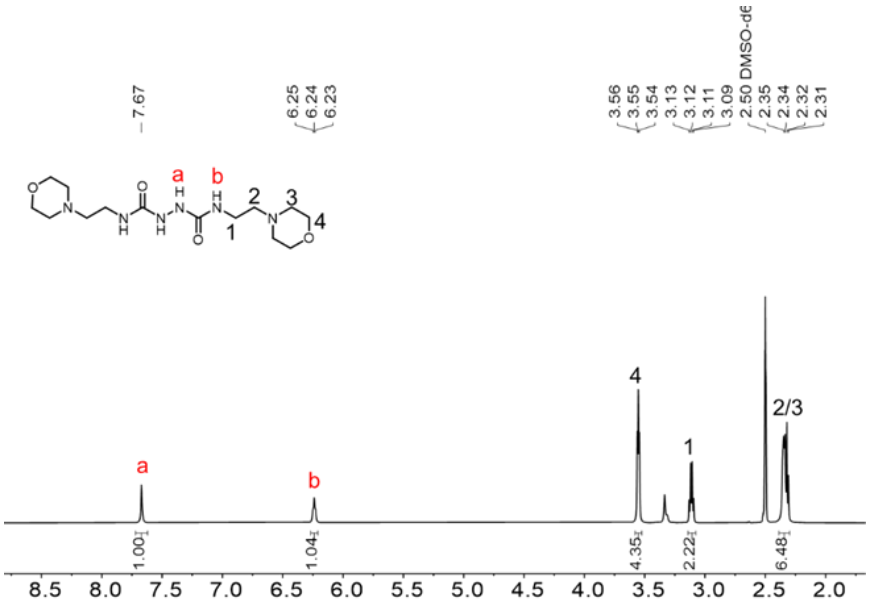

Figure S8 ^{1}H NMR spectrum of **1** (400 MHz, 298 K, DMSO-d_6).

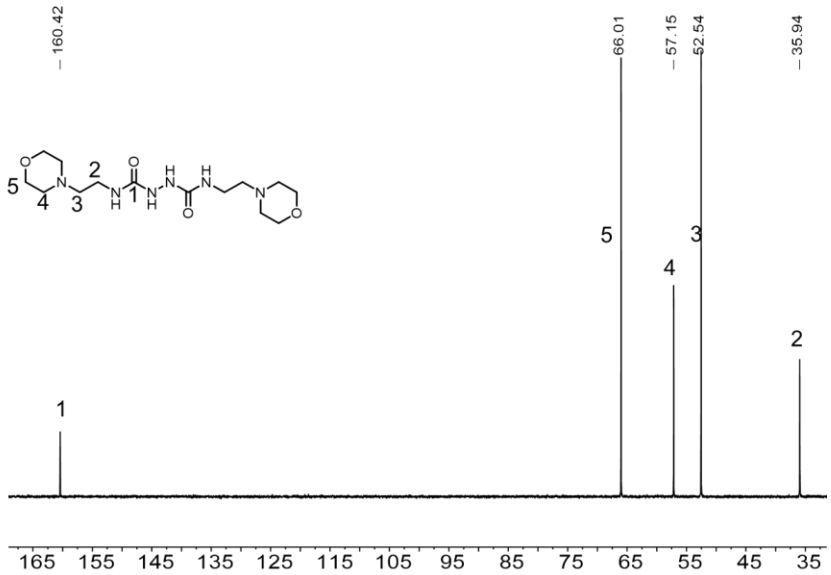

Figure S9 ^{13}C NMR spectrum of **1** (101 MHz, 298 K, DMSO-d_6).

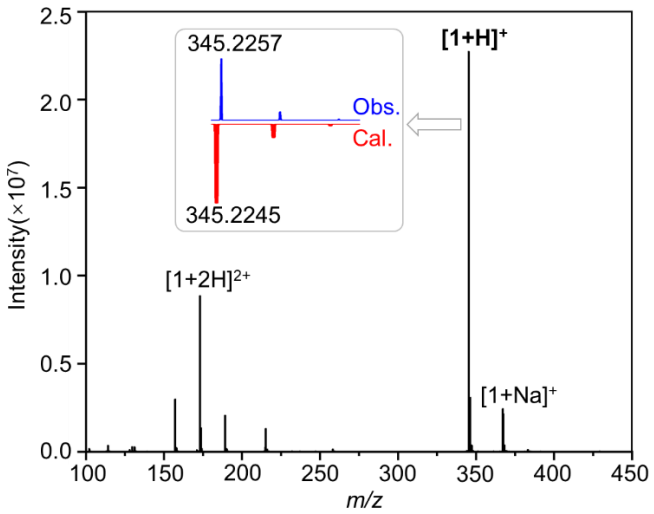

Figure S10 HR-ESI-QTOF Mass spectrum for **1**.

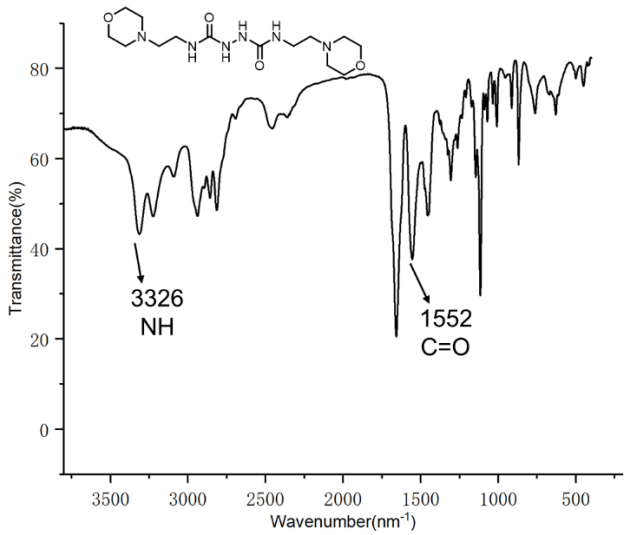

Figure S11 FT-IR spectra of **1**.

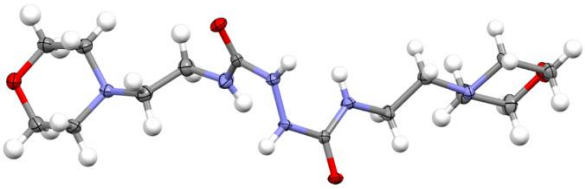

Figure S12 Single crystal structure of **1**. CCDC reference number 2517603.

Receptor 2: Compound a (1.64 g, 5.6 mmol, 3.2 equiv.) was placed in a 500 mL double-necked, round-bottomed flask and suspend in dry acetonitrile (100 mL). The reaction was heated to 50 ℃, and tris(2-aminoethyl)amine (tren, 0.25 g, 1.75 mmol, 1 equiv.) in dry acetonitrile (15 mL) was added dropwise over 30 min. The mixture was stirred at the same temperature for 24 hours. The

reaction mixture was cooled down to room temperature, and the precipitated solids was separated by filtration. The obtained white powder was further washed with acetonitrile and diethyl ether 3 times (30 mL). A white solid powder was yielded as receptor 2(Yield: 0.86 g, 80 %). ^{1}H NMR (500 MHz, DMSO-d_6) δ = 5.98 (t, J = 5.6 Hz, 1H), 5.82 (t, J = 5.6 Hz, 1H), 3.56 (t, J = 3.6 Hz, 4H), 3.10 (q, J = 6.1 Hz, 2H), 3.01 (q, J = 6.2 Hz, 2H), 2.42 (t, J = 6.5 Hz, 2H), 2.35 (s, 2H), 2.30 (t, J = 6.5 Hz, 4H). ^{13}C NMR (101 MHz, DMSO-d_6, 298 K) δ = 163.4, 72.6, 59.0, 56.2, 54.2, 38.0.

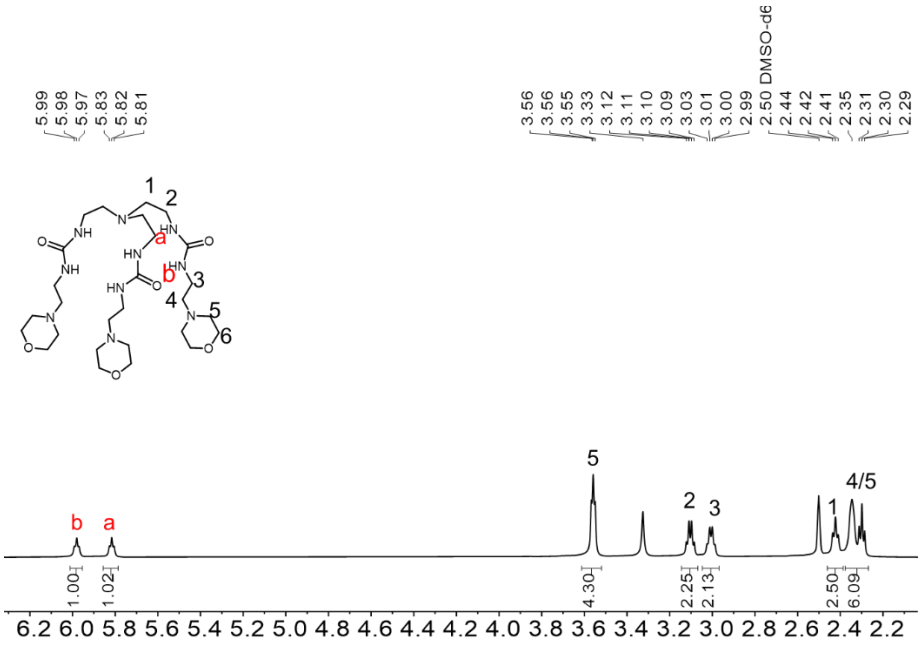

Figure S13 ^{1}H NMR spectrum of **2** (500 MHz, 298 K, DMSO-d_6).

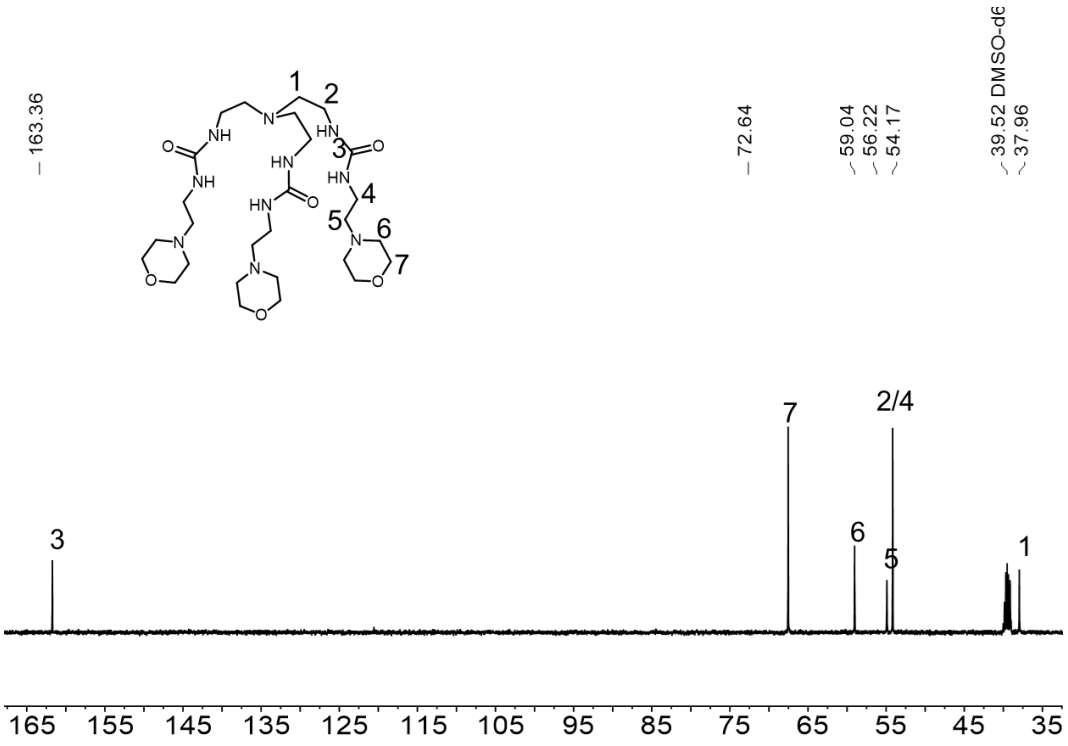

Figure S14 ^{13}C NMR spectrum of **2** (101 MHz, 298 K, DMSO-d_6).

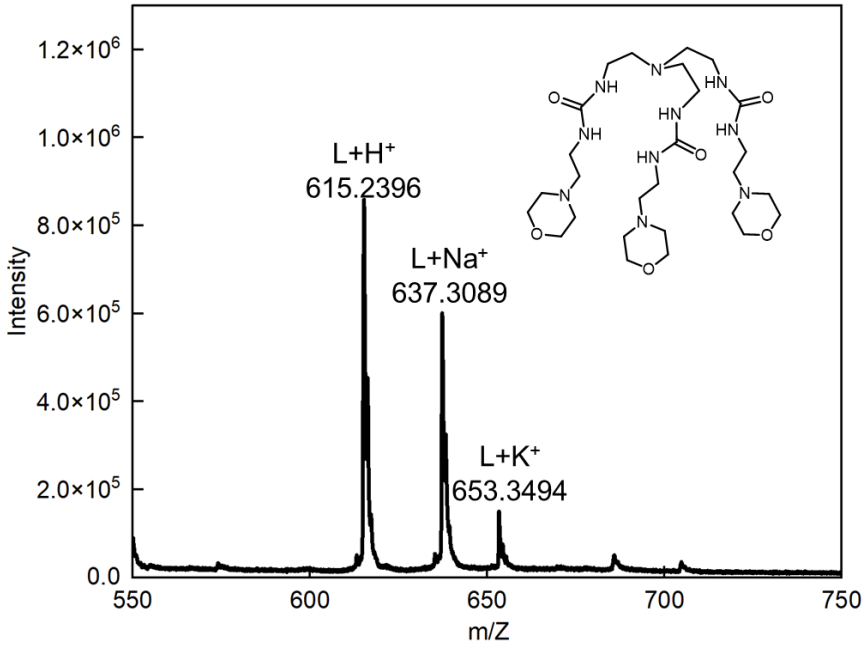

Figure S15 MALDI-QTOF spectrum for **2**.

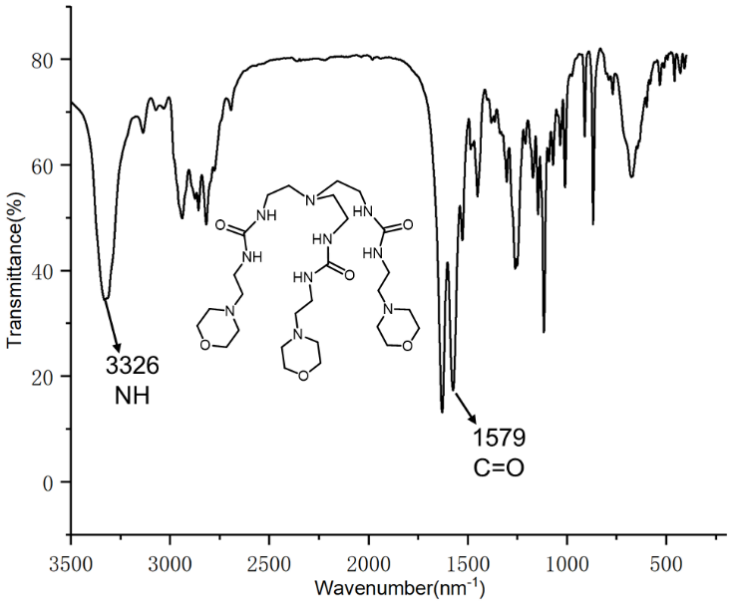

Figure S16 FT-IR spectra of **2**.

S3. CO_2 Capture and Recovery of Receptor $\mathbf{1}^{NO2}$

Capture Experiment: A 20 mL sample vial was charged with compound $\mathbf{1}^{NO2}$ (0.040 g, 0.11 mmol, 1.0 equiv.) and 40% aqueous tetramethylammonium hydroxide (TMAOH) solution (0.075 g, 0.33 mmol, 3.0 equiv.). Acetonitrile (12 mL) was added, and compound $\mathbf{1}^{NO2}$ dissolved completely to afford a black solution. When carbon dioxide (CO_2) was bubbled through the solution, the color shifted from black to orange-red. Subsequent continuous bubbling of CO_2 converted the orange-red solution to pale yellow, with the simultaneous precipitation of a white solid. Nuclear magnetic resonance (NMR) spectroscopy and mass spectrometry (MS) characterizations confirmed that the white solid was the complex of $\mathbf{1}^{NO2}$ with tetramethylammonium bicarbonate ($TMAHCO_3$), subsequently, replace this white solid with $\mathbf{1}^{NO2}$-HCO_3^-.

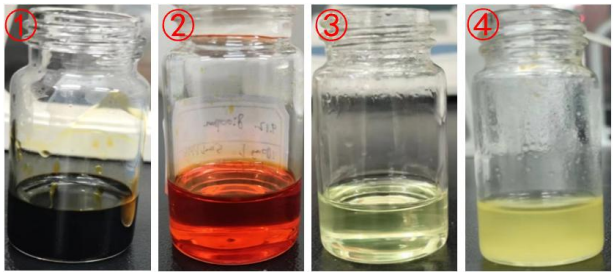

Figure S17 Changes in the system state during the CO_2 capture process.

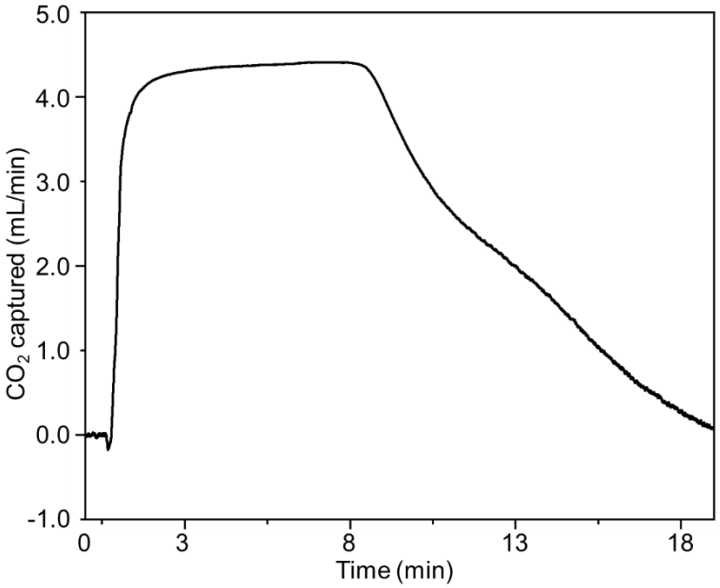

Figure S18 Representative CO_2-loading curves for $\mathbf{1}^{NO2}$.

As recorded by the CO_2 sensor, the amount of captured CO_2 increased gradually and reached a plateau within ca. 19 minutes. The determined CO_2 capacity reached 50.6 mL.

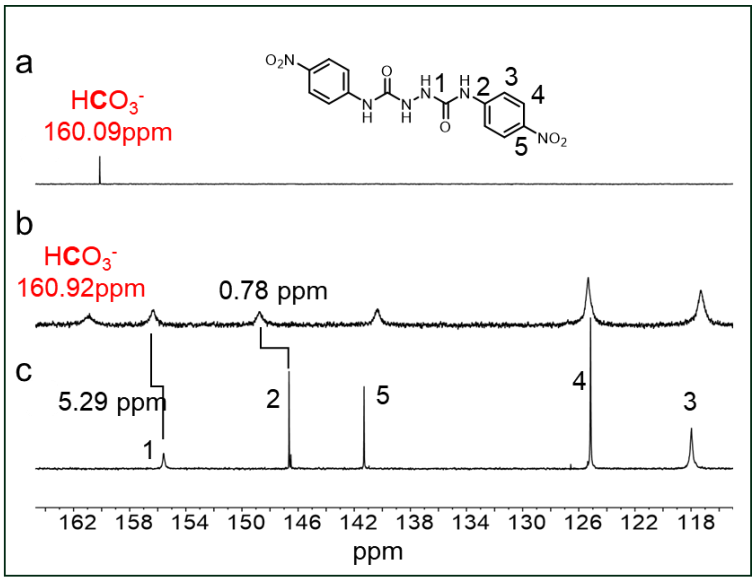

Figure S19 Stacked ^{13}C NMR spectra (500 MHz, 298 K, DMSO-d_6) of (a) $TMAHCO_3$, (b) $\mathbf{1}^{NO2}$-HCO_3^- and (c) receptor $\mathbf{1}^{NO2}$.

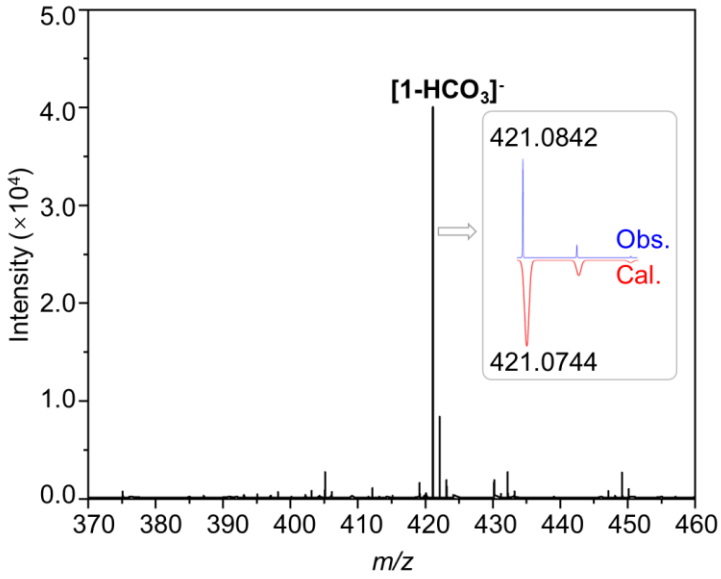

Figure S20 HR-ESI-QTOF Mass spectrum for $\mathbf{1}^{NO2}$-HCO_3^-.

The ^{13}C NMR spectra support the existence of HCO_3^- anion. New peak appeared at 160.92 ppm for $\mathbf{1}^{NO2}$, which was assigned to the HCO_3^- and consistent with reported data from literatures. The sharp signal at 160.09 ppm in the free $TMAHCO_3$ shifted to 160.92 ppm ($\Delta\delta$ = 0.83 ppm) after binding to the receptor (Figure S19), indicating the encapsulation of HCO_3^- in the receptor's cavity. Additionally, carbon adjacent to the urea functional group in the receptor showed downfield shifts, consistent with the potential hydrogen bonding with HCO_3^- anion. In addition, the white solid was analysed by ESI-QTOF mass spectrometry. Distinct peaks were observed at 421.08, assigned to

the adducts of [$\mathbf{1}^{NO2}$ + HCO_3]$^-$, respectively (Figure S20), providing direct evidence for the formation of bicarbonate complexes. The MS results combined with NMR data to support the absorption of CO_2 as the HCO_3^- anion binding complexes with receptors.

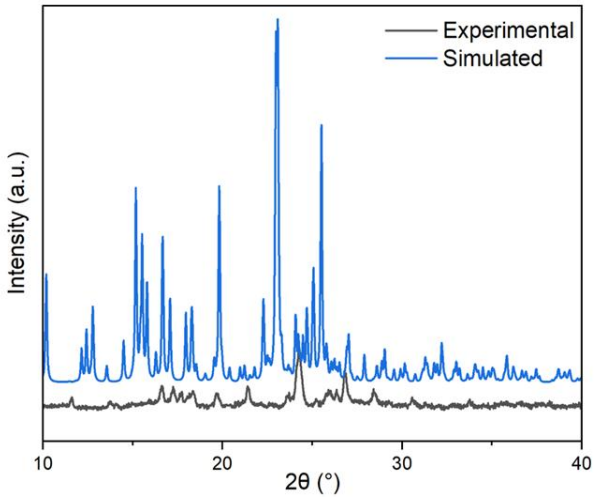

Figure S21 PXRD patterns of precipitate and the crystal structures simulated.

To investigate whether the precipitate was crystalline or amorphous, powder X-ray diffraction (PXRD) experiments were conducted on a Bruker D8 Advance diffractometer with Cu Kα radiation. The data were collected in the 2θ range of 5°–60° at a scanning rate of 5° min^{-1} under room temperature. The results revealed that the precipitate was partially amorphous rather than fully crystalline.

$\mathbf{1}^{NO2}$ Recovery: After collecting the obtained **$\mathbf{1}^{NO2}$**-HCO_3^- complex, 25 mg of the complex (Mw = 428, 0.058 mM) was dissolved in 1 mL of methanol, whereupon the complex dissolved completely. Subsequently, 5 mL of water was added, resulting in the precipitation of a yellow solid. This solid was collected, centrifuged, and dried, as shown in the figure S21.

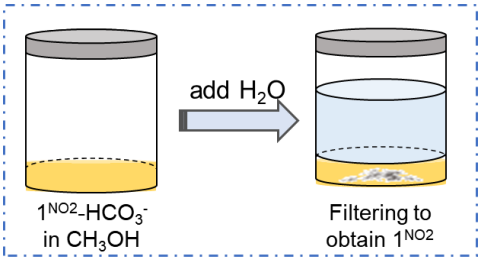

Figure S22 Schematic diagram of the process for recovering receptors using methanol: water (v: v = 1:5).

Weigh the empty centrifuge tube and the centrifuge tube after recovering the receptor. Subtract the two weights to obtain the mass of the recovered receptor, which is 19 mg (Mw = 360,

0.053 mM), with a recovery rate of 90.3%. Experimental data for CO_2 capture and receptor recovery are shown in Table S1.

Table S1 CO_2 capture and recovery of receptor.

CO_2 capture		Recovery of $\mathbf{1}^{NO2}$	
Initial wt. of $\mathbf{1}^{NO2}$(MW=360.08)	60 mg (0.167 mmol)	Wt. of $\mathbf{1}^{NO2}$-HCO_3^- complex	25 mg
Vol. of TMAOH added	320 μL	Vol of H_2O added	5 mL
Vol. of CH_3CN added	12 mL	Wt. of free $\mathbf{1}^{NO2}$	19 mg
Wt. of $\mathbf{1}^{NO2}$-HCO_3^- complex	68 mg	% of recovery (Based on $\mathbf{1}^{NO2}$)	90.3 %
% of capture on $\mathbf{1}^{NO2}$)	95.2 %		

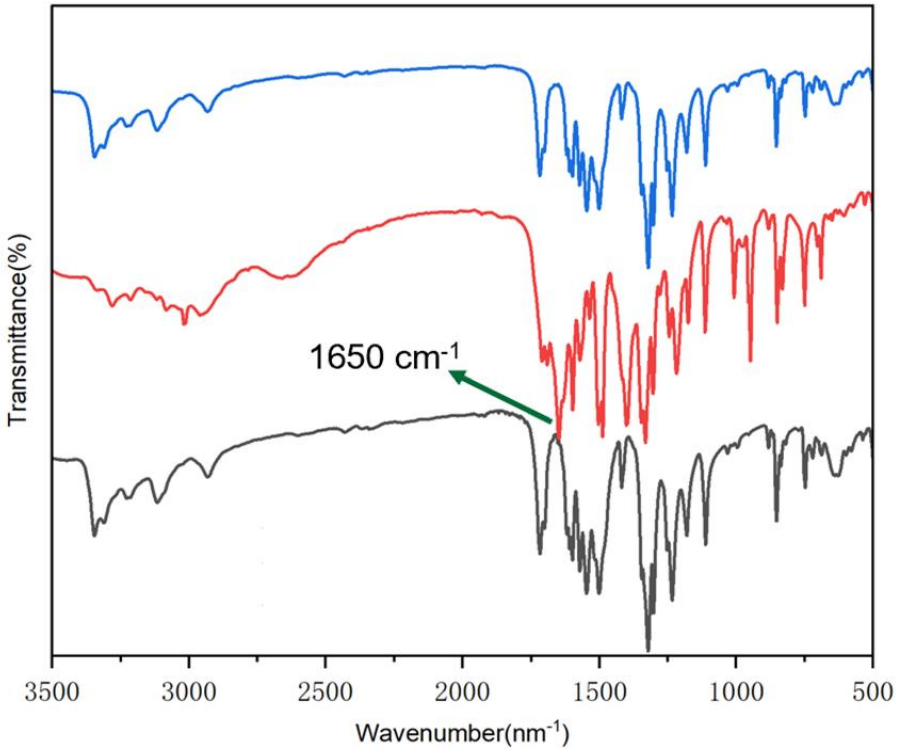

Figure S23 FT-IR spectra of receptor $\mathbf{1}^{NO2}$ (black) ,$\mathbf{1}^{NO2}$-HCO_3^- complex (red) and recovered receptor (blue).

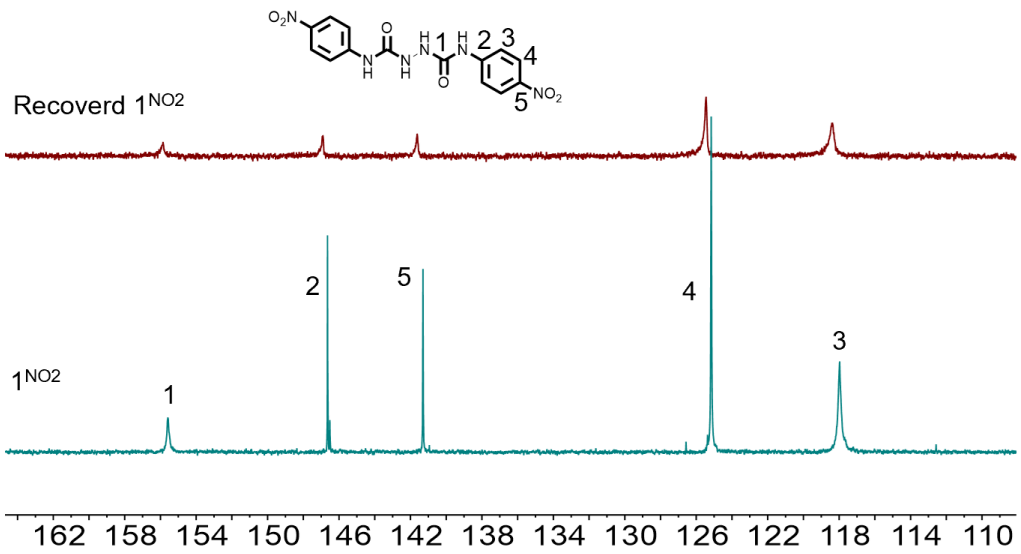

Figure S24 Stacked ^{13}C NMR spectra (500 MHz, 298 K, DMSO-d_6) of receptor and recovered receptor.

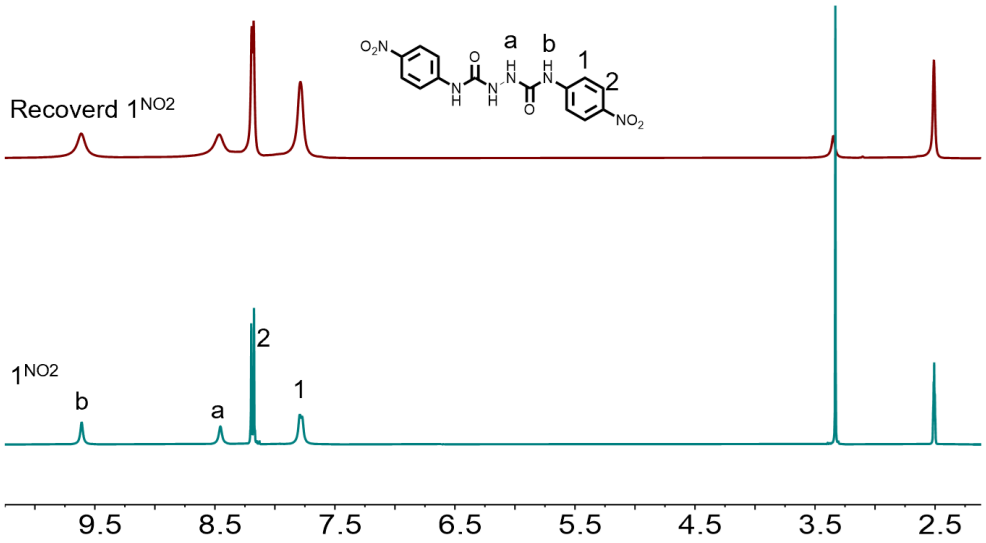

Figure S25 Stacked ^{1}H NMR spectra (500 MHz, 298 K, DMSO-d_6) of receptor and recovered receptor.

According to NMR and IR spectra (Figure S22-24), the receptor recovered using the methanol: water 1:5 method matched the IR and NMR spectra of the unused receptor, indicating that this method can be used to recover the receptor. IR spectra (Figure S22) of this isolated solid showed a spectrum (blue) which matches with the IR spectrum of **1^{NO2}** (black) indicating the clean regeneration of **1^{NO2}** under mild conditions. Simultaneously, the C=O stretching vibration peak at 1650 cm^{-1} attributable to HCO_3^- also indicates receptor regeneration.

S4. CO_2 Capture of Receptor **1** and **2**

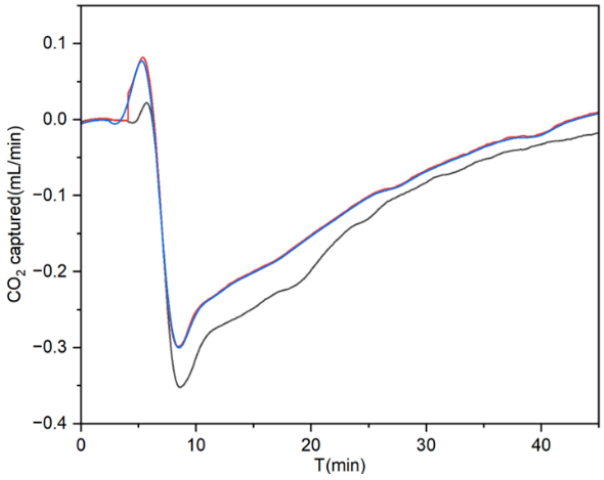

Figure S26 The amount of CO_2 captured by using receptor **1**(gas input: 10% CO_2, 90% N_2; receptor solution: [receptor] = 20 mM, H_2O, room temperature).

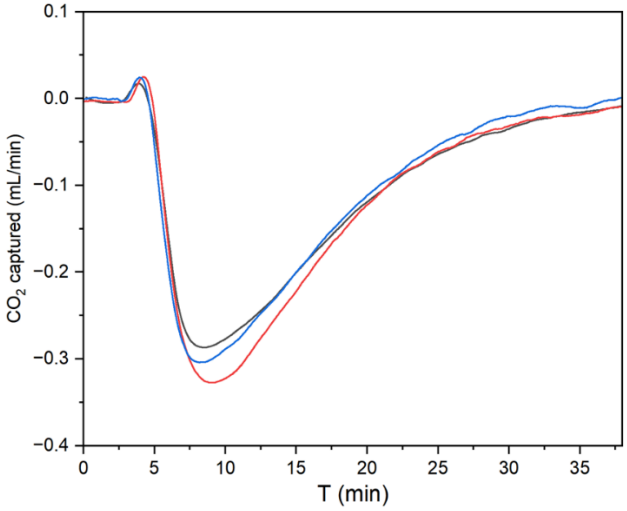

Figure S27 The amount of CO_2 captured by using receptor **2**(gas input: 10% CO_2, 90% N_2; receptor solution: [receptor] = 20 mM, H_2O, room temperature).

Determination of pKa The pKa of **1** and **2** was determined by potentiometric titration. potentiometric titration: The pKa values of **1** and **2** were determined by a pH meter. The pH of **1** (2.5mM, 2mL) and **2** (2.5mM, 2mL) aqueous solution was adjusted to 13 by NaOH, then titrated with HCl (0.375 mol/L), and the pH change was monitored with a pH meter. Through the Figure S28, the pKa value of **1** is 6.38, while that of compound **2** is 6.34.

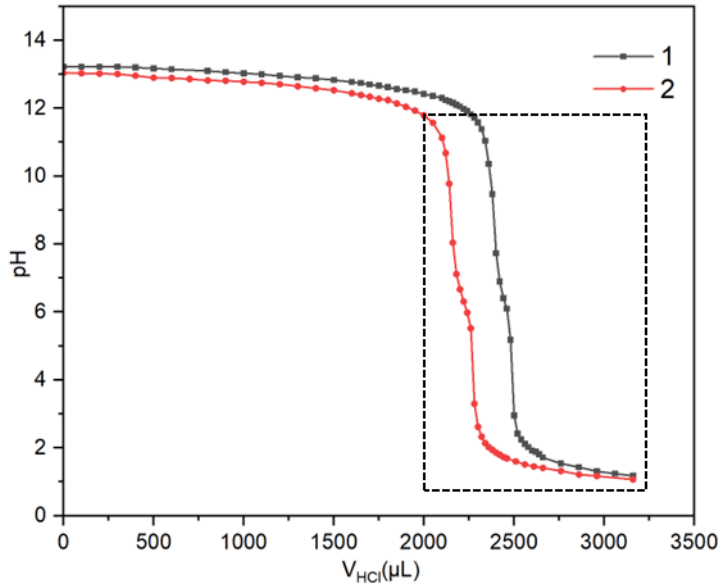

Figure S28 Potentiometric titration of **1** and **2**.

Calculating receptor capture capacity using pKa and initial/final solution pH (take a pH change of 1 as an example):

1. Calculate the protonation fractions at initial and final states

Henderson-Hasselbalch equation: pH = pKa + $\log_{10}(\frac{[amine]}{[amine^+]})$

Define the protonation fraction α = ($\frac{[amine]}{[amine]+[amine^+]}$), then: α = $\frac{1}{1+10^{pH-pKa}}$

Initial state (pH = 8.96): $\alpha_1 \approx 0.0026$ Final state (pH = 6.77): $\alpha_2 = 0.2$

Since the receptor possesses two morpholine groups capable of protonation, the total change in protonation amount is

$\Delta n = C_L \times V \times (\alpha_2-\alpha_1) \times 2 = 0.1724$ mmol

2. Relationship between CO_2 Capture and Protonation Amount

During CO_2 capture by the receptor, each mole of CO_2 absorbed is typically accompanied by the release of one mole of H^+ release (e.g., reaction: L + CO_2 + H_2O ⇌ L^--H^+ + HCO_3^-). Thus, the increase in protonation (Δn) corresponding to CO_2 capture (n_{CO2}) is: $n_{CO2} = \Delta n = 0.1724$ mmol.

This corresponds to a volume of approximately 3.86 mL under standard conditions, equivalent to 0.57 mol CO_2/mol L.

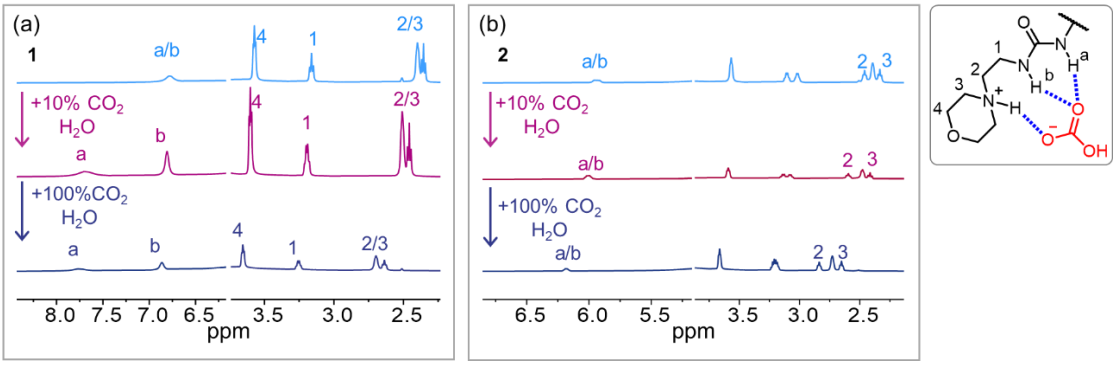

Figure S29 ^{1}H NMR spectra of receptors (a) **1** and (b) **2** before and after CO_2 capture (10% DMSO-d_6/90% H_2O, 298 K).

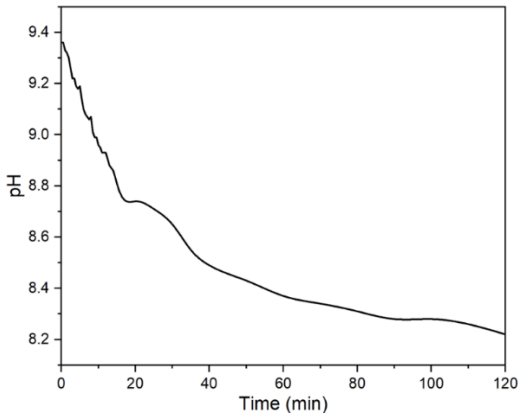

Figure S30 The pH changes by using receptors **1**.

To explore the direct air capture (DAC) capability of the receptor, we conducted direct air capture experiments accordingly. At room temperature, compressed air was bubbled through a 15 mL aqueous solution of receptor **1** with a concentration of 20 mM. The initial pH value of the receptor **1** solution was measured to be 9.36, and after gas bubbling, the pH value decreased to 8.22. This distinct pH variation serves as direct evidence confirming that the direct air capture process has occurred. Based on the pH change, the capture capacity of receptor **1** was calculated to be 0.0264 mol per mole of receptor (0.0264 mol/mol receptor, equivalent to 0.115 mmol/g). Unfortunately, we found that the absorption capacity of this receptor is far lower than that of MEA in direct air capture (DAC). This discrepancy can be primarily attributed to their distinct reaction mechanisms. Specifically, MEA reacts with to predominantly form a carbamate structure, which features strong chemical bonding and thus is highly favorable for DAC applications. In contrast, the receptor relies mainly on hydrogen bonding and electrostatic interactions to drive absorption. Owing to the relatively weak binding affinity of these non-covalent interactions, the absorption capacity of the receptor fails to meet the requirements for practical direct air capture.

S5. Recovery of Receptor **1** and **2**

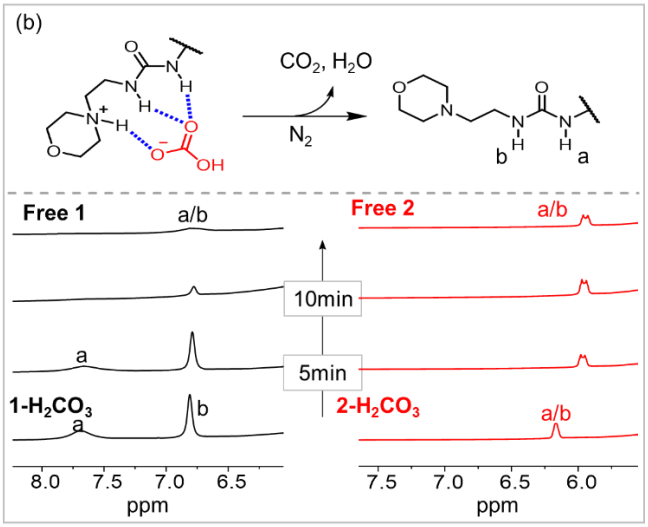

Figure S31 Stacked ^{1}H NMR N_2-swept spectra of **1**-H_2CO_3 and **2**-H_2CO_3.

S6. Single Crystal X-ray Diffraction Structures

Table S2 Crystal data details for **1**^{NO2}.

Complex	**1**^{NO2}
Empirical formula	$C_9H_{12}N_3O_4S$
Formula weight	258.28
Temperature/K	180.00
Crystal system	monoclinic
Space group	C2/c
a/Å	21.455(7)
b/Å	5.2126(19)
c/Å	21.007(8)
α/°	90
β/°	104.830(10)
γ/°	90
Volume/Å^3	2271.1(14)
Z	8
ρ_{calc}g/cm^3	1.511
μ/mm^{-1}	0.293
F(000)	1080.0
Crystal size/mm^3	0.19 × 0.12 × 0.09
Radiation	MoKα (λ = 0.71073)
2Θ range for data collection/°	4.844 to 53.676
Index ranges	-26 ≤ h ≤ 26, -5 ≤ k ≤ 6, -26 ≤ l ≤ 26
Reflections collected	15658
Independent reflections	2432 [R_{int} = 0.2333, R_{sigma} = 0.1640]
Data/restraints/parameters	2432/0/176
Goodness-of-fit on F^2	0.984
Final R indexes [I>=2σ (I)]	R_1 = 0.0655, wR_2 = 0.1291
Final R indexes [all data]	R_1 = 0.1726, wR_2 = 0.1618
Largest diff. peak/hole / e Å^{-3}	0.32/-0.46

Table S3 Crystal data details for **1**.

Complex	**1**
Empirical formula	$C_{14}H_{28}N_6O_4$
Formula weight	344.42
Temperature/K	180.00
Crystal system	triclinic
Space group	P-1
a/Å	5.5769(13)
b/Å	9.0107(18)
c/Å	17.242(4)
α/°	84.098(6)
β/°	89.986(7)
γ/°	87.342(7)
Volume/Å^3	860.9(3)
Z	2
ρ_{calc}g/cm^3	1.329
μ/mm^{-1}	0.099
F(000)	372
Crystal size/mm^3	0.19 × 0.12 × 0.09
Radiation	MoKα (λ = 0.71073)
2Θ range for data collection/°	4.75 to 50.92
Index ranges	-6 ≤ h ≤ 6, -10 ≤ k ≤ 10, -20 ≤ l ≤ 20
Reflections collected	9955
Independent reflections	3164 [R_{int} = 0.1069, R_{sigma} = 0.1254]
Goodness-of-fit on F^2	0.995
Final R indexes [I>=2σ (I)]	R_1 = 0.0568, wR_2 = 0.1192
Final R indexes [all data]	R_1 = 0.1311, wR_2 = 0.1434
Largest diff. peak/hole / e Å^{-3}	0.41/-0.44

Table S4 Crystal data details for $\mathbf{1}^{NO2}$-HCO_3^-.

Complex	$\mathbf{1}^{NO2}$-HCO_3^-
Empirical formula	$C_{38}H_{50}N_{14}O_{18}$
Formula weight	990.92
Temperature/K	180.00
Crystal system	monoclinic
Space group	C2/c
a/Å	33.884(5)
b/Å	7.6616(10)
c/Å	20.711(3)
α/°	90
β/°	121.710(4)
γ/°	90
Volume/Å^3	4574.1(10)
Z	4
ρ_{calc}g/cm^3	1.439
μ/mm^{-1}	0.116
F(000)	2080.0
Crystal size/mm^3	0.19 × 0.12 × 0.17
Radiation	MoKα (λ = 0.71073)
2Θ range for data collection/°	4.624 to 50.256
Index ranges	-39 ≤ h ≤ 40, -9 ≤ k ≤ 9, -24 ≤ l ≤ 24
Reflections collected	24936
Independent reflections	4069 [R_{int} = 0.0805, R_{sigma} = 0.0471]
Goodness-of-fit on F^2	1.043
Final R indexes [I>=2σ (I)]	R_1 = 0.0722, wR_2 = 0.1691
Final R indexes [all data]	R_1 = 0.1091, wR_2 = 0.1959
Largest diff. peak/hole / e Å^{-3}	0.51/-0.42

Table S5 Crystal data details for $\mathbf{1}^{NO2}$-CO_3^{2-}.

Complex	$\mathbf{1}^{NO2}$-CO_3^{2-}
Empirical formula	$C_{47.4}H_{68.8}N_{14}O_{17.6}$
Formula weight	1116.36
Temperature/K	180.00
Crystal system	monoclinic
Space group	C2/m
a/Å	20.964(10)
b/Å	18.802(8)
c/Å	7.305(4)
α/°	90
β/°	91.246(11)
γ/°	90
Volume/Å^3	2879(2)
Z	2
ρ_{calc}g/cm^3	1.288
μ/mm^{-1}	0.100
F(000)	1184.0
Crystal size/mm^3	0.19 × 0.12 × 0.12
Radiation	MoKα (λ = 0.71073)
2Θ range for data collection/°	4.332 to 37.858
Index ranges	-19 ≤ h ≤ 19, -17 ≤ k ≤ 17, -6 ≤ l ≤ 6
Reflections collected	8070
Independent reflections	1202 [R_{int} = 0.1496, R_{sigma} = 0.0733]
Goodness-of-fit on F^2	1.037
Final R indexes [I>=2σ (I)]	R_1 = 0.0841, wR_2 = 0.2020
Final R indexes [all data]	R_1 = 0.1208, wR_2 = 0.2274
Largest diff. peak/hole / e Å^{-3}	0.32/-0.30

X-ray diffraction data were collected on a Bruker D8 Venture Photon II diffractometer at 180 K with graphite-monochromated Mo Kα radiation (λ = 0.71073 Å). An empirical absorption correction using SADABS was applied for all data (G. M. Sheldrick, Program SADABS: Area Detector Absorption Correction, 1996, University of Göttingen, Germany). The structures were solved by the dual methods using the SHELXS program (G. Sheldrick, Acta Cryst. A, 2008, 64, 5 112-122). All non-hydrogen atoms were refined anisotropically by full-matrix least-squares on F2 using the program SHELXL, and hydrogen atoms were included in idealized positions with thermal

parameters equivalent to 1.2 times those of the atom to which they were attached. Some remaining solvents could not be successfully resolved despite numerous attempts at modeling, and consequently the SQUEEZE function of PLATON was used to account for these highly disordered solvents.

Table S6 Hydrogen bonding information in the crystal structure of **1**^{NO2}.

	d (D-H) Å	*d* (H···A) Å	*d* (D···A) Å	∠DHA
N1-H1···O7	0.88	2.13	2.867(4)	141°
N2-H2···O7	0.88(4)	2.13(4)	2.976(5)	161°
N2-H2···O1	0.88(4)	2.38(4)	2.727(5)	103°

Table S7 Hydrogen bonding information in the crystal structure of **1**.

	d (D-H) Å	*d* (H···A) Å	*d* (D···A) Å	∠DHA
N5-H5···O2	0.88	2.30	2.972(3)	134°
N7-H7···N5	0.88	2.36	2.718(3)	105°
N7-H7···O2	0.88	2.25	3.001(3)	143°
N8-H8···O1	0.88	2.08	2.901(3)	156°
N6-H6···O1	0.88	2.38	3.196(3)	154°

Table S8 Hydrogen bonding information in the crystal structure of **1**^{NO2}-HCO_3^-.

	d (D-H) Å	*d* (H···A) Å	*d* (D···A) Å	∠DHA
N4-H4···O2	0.84	1.76	2.597(4)	175°
N6-H6···O2	0.88	1.96	2.827(3)	169°
N7-H7···O3	0.88	2.16	3.025(4)	167°
N7-H7···N9	0.88	2.28	2.654(5)	105°

N8-H8···O2	0.88	2.45	3.198(4)	143°
N8-H8···O3	0.88	2.02	2.803(4)	148°

Table S9 Hydrogen bonding information in the crystal structure of **1**^{NO2}-CO_3^{2-}.

	d (D-H) Å	*d* (H···A) Å	*d* (D···A) Å	∠DHA
N1-H1···O2	0.88	2.22	2.891(5)	133°
N1-H1···O5	0.88	1.98	2.832(4)	163°
N1-H1···O3	0.88	2.04	2.722(5)	133°
N1-H1···O5	0.88	1.84	2.681(4)	160°
N4-H4···O2	0.88	2.13	2.923(4)	149°
N4-H4···O3	0.88	2.04	2.912(4)	172°
N4-H4···O2	0.88	1.89	2.774(4)	174°
N4-H4···O3	0.88	1.91	2.711(4)	149°